Computer Physics Communications 287 (2023) 108697

Contents lists available at ScienceDirect

Computer Physics Communications

journal homepage: www.elsevier.com/locate/cpc

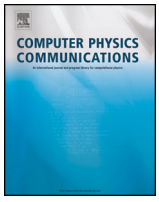

SBETHE: Stopping powers of materials for swift charged particles from the corrected Bethe formula ☆,☆☆

Francesc Salvat [a,*], Pedro Andreo [b]

[a] Facultat de Física (FQA and ICC), Universitat de Barcelona, Diagonal 645, 08028 Barcelona, Catalonia, Spain
[b] Department of Medical Radiation Physics and Nuclear Medicine, Karolinska University Hospital, SE-17176 Stockholm, Sweden

ARTICLE INFO

Article history:
Received 25 November 2022
Received in revised form 1 February 2023
Accepted 11 February 2023
Available online 24 February 2023

Keywords:
Stopping power
Corrected Bethe formula
Inelastic collisions of charged particles
Bremsstrahlung emission by electrons
Plane-wave Born approximation

ABSTRACT

The Fortran program SBETHE calculates the stopping power of materials for swift charged particles with small charges (electrons, muons, protons, their antiparticles, and alphas). The electronic stopping power is computed from the corrected Bethe formula, with the shell correction derived from numerical calculations with the plane-wave Born approximation (PWBA) for atoms, which were based on an independent-electron model with the Dirac–Hartree–Fock–Slater self-consistent potential for the ground-state configuration of the target atom. The density effect correction is evaluated from an empirical optical oscillator strength (OOS) model based on atomic subshell contributions obtained from PWBA calculations. For projectiles heavier than the electron, the Barkas correction is evaluated from the OOS model, and the Lindhard–Sørensen correction is estimated from an accurate parameterization of its numerical values. The calculated electronic stopping power is completely determined by a single empirical parameter, the mean excitation energy or I value of the material. The radiative stopping power for electrons, and positrons, is evaluated by means of Seltzer and Berger's cross section tables for bremsstrahlung emission. The program yields reliable stopping powers and particle ranges for arbitrary materials and projectiles with kinetic energy larger than a certain cutoff value $E_{\rm cut}$, which is specific of each projectile kind. The program is accompanied by an extensive database that contains tables of relevant energy-dependent atomic quantities for all the elements from hydrogen to einsteinium. `sbethe` may be used to generate basic information for dosimetry calculations and Monte Carlo simulations of radiation transport, and as a pedagogical tool.

Program summary

Program title: SBETHE
CPC Library link to program files: https://doi.org/10.17632/7zw25f428t.1
Licensing provisions: CC by NC 3.0
Programming language: Fortran 90/95
Nature of problem: The program calculates the stopping power of arbitrary materials for swift charged projectiles with small charges. The material is characterized by its chemical composition, mass density, and the empirical I value. The considered projectiles are electrons, positrons, negative muons, antimuons, protons, antiprotons, and alphas, which are described as point particles characterized by their mass and charge. If the actual I value of the material is known, the results from the program are expected to be reliable for projectiles with kinetic energy higher than a value $E_{\rm cut}$, of the order of 1 keV for electrons and positrons, 150 keV for muons and antimuons, 0.75 MeV for protons and antiprotons, and 5 MeV for alpha particles.
Solution method: The electronic stopping power is calculated by means of a corrected Bethe formula [1], which combines the conventional Bethe logarithm with the following corrections,
1) the shell correction obtained from calculations based on the plane-wave Born approximation with the self-consistent Dirac–Hartree–Fock–Slater (DHFS) potential of neutral atoms in their ground-state configuration [2],
2) the density effect correction, which accounts for the reduction of the stopping power caused by the

☆ The review of this paper was arranged by Prof. Z. Was.
☆☆ This paper and its associated computer program are available via the Computer Physics Communications homepage on ScienceDirect (http://www.sciencedirect.com/science/journal/00104655).

* Corresponding author.
E-mail address: francesc.salvat@ub.edu (F. Salvat).

https://doi.org/10.1016/j.cpc.2023.108697

dielectric polarization of the medium,
3) a parameterization of the Lindhard–Sørensen correction, which generalizes the Bloch correction for relativistic projectiles, and
4) the Barkas correction, which accounts for differences between the stopping powers of particles and their antiparticles.
The density-effect and the Barkas corrections are calculated from a model of the optical oscillator strength (OOS) of the material, which combines the contributions of inner atomic subshells calculated with the DHFS potential, with a classical oscillator model for the contribution of valence electrons,
A simple extrapolation formula is used to extend the calculated electronic stopping power to energies less than E_{cut} to allow the calculation of particle ranges.
For electrons and positrons, the radiative stopping power is calculated from numerical tables prepared by Seltzer and Berger [3].
Additional comments including restrictions and unusual features: The calculated stopping power is determined by a single parameter, the mean excitation energy or I value. The program assigns to each material a default I value, derived from the recommendations in the ICRU Report 37, which can be changed by the user. The distribution package includes text files with tables of atomic energy-dependent quantities (subshell optical oscillator strengths, shell corrections, scaled cross sections for bremsstrahlung emission) that are used in the calculations.

References

[1] F. Salvat, Phys. Rev. A 106 (2022) 032809.
[2] F. Salvat, L. Barjuan, P. Andreo, Phys. Rev. A 105 (2022) 042813.
[3] S.M. Seltzer, M.J. Berger, Nucl. Instrum. Methods B 12 (1985) 95–134.

1. Introduction

The stopping power of materials for swift charged particles [1,2] is a fundamental quantity in dosimetry studies and in Monte Carlo simulations of radiation transport. The stopping power is defined as the average energy loss per unit path length of the projectile. In spite of its practical importance, the available sources of reliable stopping power tables are essentially limited to the Reports of the International Commission on radiation Units and Measurements (ICRU) [3–5] and various unpublished computer codes associated to those Reports. Frequently the stopping power is estimated from the uncorrected Bethe formula, even when the energy of the projectile is below the validity limit of that formula.

Fast charged projectiles lose energy though interactions of different kinds, namely, 1) inelastic collisions, *i.e.*, interactions that produce electronic excitations of the material (electronic stopping), 2) elastic collisions, which cause the recoil of the target atom (nuclear stopping), and 3) the emission of bremsstrahlung, or breaking radiation (radiative stopping). The latter is negligible for particles heavier than the electron. Nuclear stopping, which is appreciable only for particles heavier than the electron that move with small speeds, is not considered.

The present article describes the computer program SBETHE that calculates the stopping power of materials for fast charged particles from the most reliable theoretical and semiempirical approaches available. The considered projectiles are electrons, positrons, negative muons, antimuons, protons, antiprotons, and alphas; they are all treated as charged point particles. The radiative stopping power for electrons, and positrons, is evaluated from the tables of atomic cross sections for bremsstrahlung emission prepared by Seltzer and Berger [6,7]. The electronic stopping power is calculated from the corrected Bethe formula, as described by Salvat [8]. In principle, the Bethe formula approximates the results obtained from the plane-wave Born approximation (PWBA) for thin gases only asymptotically, *i.e.*, for projectiles with very large kinetic energies. The shell correction, the density-effect correction, the Lindhard–Sørensen correction, and the Barkas correction are introduced so as to extend the validity of the formula to condensed materials and to projectiles with moderately low kinetic energies. However, the calculation of these corrections is far from trivial and, more importantly, it requires knowledge of the optical-oscillator strength (OOS) of the material and other energy-dependent quantities, which are not generally available. The calculation scheme implemented in SBETHE combines pre-calculated atomic data with an empirical model of the OOS built from atomic subshell OOS that is determined by the adopted empirical value of the mean excitation energy, or I value, of the material. The corrected Bethe formula allows calculating the electronic stopping power only for particles with kinetic energy higher than a certain value E_{cut}, of the order of 1 keV for electrons and positrons, 150 keV for muons and antimuons, 0.75 MeV for protons and antiprotons, and 5 MeV for alpha particles. In spite of this limitation, the formula provides the stopping powers required in calculations and Monte Carlo simulations of the transport of fast charged particles with initial energies such that their initial ranges are much larger than the residual ranges at E_{cut}.

The article is organized as follows. Section 2 provides a brief description of the plane-wave Born approximation (PWBA) for inelastic collisions of charged projectiles with atoms, which is the fundamental theory underlying the Bethe formula for the stopping power. Exchange effects in inelastic collisions of electrons and positrons are accounted for by considering that collisions involving large energy transfers are correctly described by the Møller [9] and Bhabha [10] differential cross sections (DCSs) for collisions with free electrons at rest. The atomic shell correction was evaluated by requiring that the Bethe formula with that correction included yields the same stopping cross section as the numerical PWBA calculations. In Section 3, the density-effect, Lindhard–Sørensen, and Barkas corrections are introduced to obtain a corrected Bethe formula that is applicable to arbitrary materials [8] and projectiles with kinetic energy higher than E_{cut}. In order to estimate the range of projectiles with energies near E_{cut}, the results from the corrected Bethe formula are extrapolated to lower energies by using a simple analytical form that places the maximum of the electronic stopping power at nearly the same energy as the available experimental measurements. Section 4 describes the calculation of the radiative stopping power for electrons and positrons. The Fortran program SBETHE and the associated database are described in Section 5. For each kind of projectile particles and for a given material (described by its chemical composition and mass density),

the program computes detailed tables of the total stopping power (electronic plus radiative) and the average range as functions of the kinetic energy of the projectile in terms of the I-value of the material, which is proposed by the program or defined by the user. The complete calculation takes less than about one second on a modest personal computer.

In the calculations we consider a fast charged projectile (mass M_1 and charge $Z_1 e$, with e denoting the elementary charge) that moves with kinetic energy E in a homogeneous compound material with Z electrons per molecule and $\mathcal{N}$ molecules per unit volume. To cover the energy range of interest, relativistic kinematics is used. We recall that the kinetic energy E and the magnitude p of the linear momentum of the projectile can be expressed as

$$E = (\gamma - 1)\, M_1 c^2, \quad p = \beta\gamma\, M_1 c\,, \tag{1}$$

where

$$\beta = \frac{v}{c} = \sqrt{\frac{\gamma^2 - 1}{\gamma^2}} = \sqrt{\frac{E(E + 2M_1c^2)}{(E + M_1c^2)^2}} \tag{2}$$

is the projectile's velocity v in units of the speed of light c, and

$$\gamma = \sqrt{\frac{1}{1 - \beta^2}} = \frac{E + M_1c^2}{M_1c^2} \tag{3}$$

is the total energy of the projectile in units of its rest energy. Notice that

$$cp = \sqrt{E(E + 2M_1c^2)}. \tag{4}$$

2. Electronic stopping

Electronic stopping is the dominant energy-loss process for charged particles heavier than the electron. For projectile electrons and positrons electronic stopping dominates for kinetic energies less than a critical energy that, for elemental materials, decreases when the atomic number increases ($\sim$ 50 MeV, 15 MeV, and 10 MeV for aluminum, silver, and gold, respectively); above this energy, the radiative stopping power exceeds the electronic one.

Inelastic collisions of fast charged projectiles with randomly oriented atoms or molecules can be described by means of the relativistic plane-wave (first) Born approximation (PWBA) [see, *e.g.*, 1,11]. Each collision involves a certain energy transfer W from the projectile to the target and an angular deflection of the projectile, determined by the cosine of the polar scattering angle, $\cos\theta$. Let E and $\mathbf{p}$ denote the kinetic energy and linear momentum of the projectile before the collision, the corresponding quantities after the collision are denoted by primes, E' and $\mathbf{p}'$. Evidently,

$$E' = E - W \quad \text{and} \quad p' = c^{-1}\sqrt{(E - W)(E - W + 2M_1c^2)}\,. \tag{5}$$

The central result from the PWBA is a closed expression of the doubly differential cross section (DDCS) as a function of W and $\cos\theta = \hat{\mathbf{p}}\cdot\hat{\mathbf{p}}'$. This DDCS takes a cleaner form when expressed in terms of the recoil energy Q defined by [1]

$$Q\,(Q + 2m_ec^2) = c^2(\mathbf{p} - \mathbf{p}')^2 = (cp)^2 + (cp')^2 - 2c^2pp'\cos\theta\,, \tag{6}$$

where m_e is the electron mass. The DDCS for collisions leaving the target either in an excited bound state (excitation) or in a free state (ionization) is [12,13]

$$\frac{\mathrm{d}^2\sigma_{\rm in}}{\mathrm{d}W\,\mathrm{d}Q} = \frac{2\pi Z_1^2 e^4}{m_e v^2}\left[\frac{2m_ec^2}{W\,Q\,(Q + 2m_ec^2)}\right.$$
$$\times\left\{\frac{(2E - W + 2M_1c^2)^2 - Q\,(Q + 2m_ec^2)}{4\,(E + M_1c^2)^2}\right\}\frac{\mathrm{d}f(Q\,,W)}{\mathrm{d}W}$$
$$+\,\frac{2m_ec^2W}{[Q\,(Q + 2m_ec^2) - W^2]^2}$$
$$\left.\times\left(\beta^2\sin^2\theta_{\rm r} + \left\{\frac{Q\,(Q + 2m_ec^2) - W^2}{2(E + M_1c^2)^2}\right\}\right)\frac{\mathrm{d}g(Q\,,W)}{\mathrm{d}W}\right], \tag{7}$$

with

$$\beta^2\sin^2\theta_{\rm r} = \beta^2 - \frac{W^2}{Q\,(Q + 2m_ec^2)}\left(1 + \frac{Q\,(Q + 2m_ec^2) - W^2}{2W(E + M_1c^2)}\right)^2. \tag{8}$$

The factors $\mathrm{d}f(Q\,,W)/\mathrm{d}W$ and $\mathrm{d}g(Q\,,W)/\mathrm{d}W$ are, respectively, the longitudinal and transverse generalized oscillator strengths (GOSs), which completely characterize the effect of inelastic collisions on the projectile.

In the case of target atoms (or ions), the GOSs can be calculated numerically by combining the PWBA with an independent-particle model of the atomic electron cloud, *i.e.*, by assuming that atomic electrons move independently of each other under a common central potential, $V(r)$. Calculations with the self-consistent Dirac–Hartree–Fock–Slater potential for the ground-state configurations of neutral atoms have been performed by Salvat et al. [13] for all the elements of the periodic table, from hydrogen ($Z = 1$) to einsteinium ($Z = 99$). A detailed description of the underlying theory and the numerical methods employed in those calculations is given in the document `rpwba.pdf` [14]. From the calculated GOS tables one can easily obtain the atomic DDCS (7) for projectiles with arbitrary charge, mass, and kinetic energy.

In the limit $Q \to 0$ both the longitudinal and transverse GOSs reduce to the optical oscillator strength (OOS), which is an important ingredient of the corrected Bethe formula (see below),

$$\frac{\mathrm{d}f(0,W)}{\mathrm{d}W} = \frac{\mathrm{d}g(0,W)}{\mathrm{d}W} = \frac{\mathrm{d}f(W)}{\mathrm{d}W}, \tag{9}$$

while for large Q the GOSs can be approximated as

$$\frac{\mathrm{d}f(Q\,,W)}{\mathrm{d}W} = \frac{\mathrm{d}g(Q\,,W)}{\mathrm{d}W} \simeq Z\delta(Q - W), \tag{10}$$

where $\delta(x)$ is the Dirac delta distribution. The longitudinal GOS satisfies the sum rule

$$\int_0^\infty \frac{\mathrm{d}f(Q\,,W)}{\mathrm{d}W}\,\mathrm{d}W = Z\,[1 - \Delta(Q)]\,, \tag{11}$$

where $\Delta(Q)$, the departure from the non-relativistic Bethe sum rule [13], increases with Z and decreases with Q. For single atoms, the largest value of $\Delta(Q)$ is about 0.025 for $Z = 99$ and $Q = 0$.

Integration of the DDCS over recoil energies yields the energy-loss differential cross section (DCS),

$$\frac{\mathrm{d}\sigma_{\rm in}}{\mathrm{d}W} = \int_{Q_-}^{Q_+}\frac{\mathrm{d}^2\sigma_{\rm in}}{\mathrm{d}W\,\mathrm{d}Q}\,\mathrm{d}Q\,, \tag{12}$$

where $Q_\pm$ are the lower and upper limits of the kinematically allowed interval of recoil energies, corresponding to $\cos\theta = \pm 1$, that is,

$$Q_\pm(Q_\pm + 2m_ec^2) = c^2(\mathbf{p} - \mathbf{p}')^2 = (cp)^2 + (cp')^2 \pm 2c^2pp'\,,$$

or

$$Q_{\pm} = \sqrt{(cp \pm cp')^2 + m_e^2 c^4} - m_e c^2 \,. \tag{13}$$

The total cross section, $\sigma_{\rm in}^{(0)}$, and the stopping cross section, $\sigma_{\rm in}^{(1)}$, are obtained as integrals of the energy-loss DCS,

$$\sigma_{\rm in}^{(n)} = \int_0^{W_{\rm max}} W^n \, \frac{{\rm d}\sigma_{\rm in}}{{\rm d}W} \, {\rm d}W \tag{14}$$

where $W_{\rm max}$ is the largest allowed energy loss in a single collision, which is given by [8]

$$W_{\rm max} = \frac{2\beta^2\gamma^2 m_e c^2}{1 + 2(m_e/M_1)\gamma + (m_e/M_1)^2} \,. \tag{15}$$

For projectile positrons, $W_{\rm max} = (\gamma - 1) m_e c^2 = E$, while for projectile electrons $W_{\rm max} = E/2$ because of the indistinguishability between the projectile and the target electrons (see Section 2.1 below).

The electronic stopping power $S_{\rm in}$ is defined as the average energy loss per unit path length s of the projectile caused by inelastic collisions. It can be evaluated as the ratio of the average energy loss in a collision,

$$\langle W \rangle = \int_0^{W_{\rm max}} W \, \frac{1}{\sigma_{\rm in}^{(0)}} \, \frac{{\rm d}\sigma_{\rm in}}{{\rm d}W} \, {\rm d}W \,, \tag{16}$$

and the mean free path for inelastic interactions, $\lambda = (\mathcal{N}\sigma_{\rm in}^{(0)})^{-1}$, that is,

$$S_{\rm in} \equiv -\frac{{\rm d}E}{{\rm d}s} = \frac{\langle W \rangle}{\lambda} = \mathcal{N}\sigma_{\rm in}^{(1)} \,. \tag{17}$$

Very often the terms "stopping power" and "stopping cross section" are used interchangeably.

2.1. Corrections for electrons and positrons

Collisions of electrons ($Z_1 = -1$, $M_1 = m_e$) with atoms differ from those of heavier particles in that the projectile is indistinguishable from the atomic electrons and, consequently, interactions are affected by exchange effects (such as re-arrangement collisions and interference between direct and exchange transition-matrix elements). Exchange effects occur also in inelastic collisions of positrons ($Z_1 = +1$, $M_1 = m_e$). The reason is that the (active) electron-positron pair can undergo annihilation followed by recreation of a new pair, a process that coexists with ordinary scattering. Exchange effects then arise from the indistinguishability of the target electron from the electrons in virtual states of negative energy (the Dirac sea). In the energy range where the PWBA is expected to be reliable, the total cross section is known to be fairly insensitive to these effects (see, *e.g.*, Ref. [12]). However, electron exchange introduces appreciable modifications in the stopping power of both electrons and positrons.

In the present calculations, exchange effects for projectile electrons and positrons are accounted for by multiplying the DDCS by a correction factor such that the energy-loss DCS at sufficiently large W's reduces to the DCS for collisions with Z electrons at rest [14]. Explicitly, the energy-loss DCS for large-W collisions of electrons with free electrons at rest is given by the Møller formula [9]

$$\frac{{\rm d}\sigma_{\rm Møller}}{{\rm d}W} = \frac{2\pi e^4}{m_e v^2} \frac{1}{W^2} \, F_{\rm Møller}(W) \,, \tag{18}$$

where

$$F_{\rm Møller}(W) = 1 + \left(\frac{W}{E-W}\right)^2 - \frac{(1-b_0)W}{E-W} + \frac{b_0 W^2}{E^2} \tag{19}$$

with

$$b_0 = \left(\frac{E}{E + m_e c^2}\right)^2 = \left(\frac{\gamma - 1}{\gamma}\right)^2 = \left(1 - \sqrt{1-\beta^2}\right)^2 \,. \tag{20}$$

In ionizing collisions, we have two (indistinguishable) free electrons in the final state, and it is natural to consider the fastest as the "primary". Consequently, the largest allowed energy loss in binary collisions of electrons is

$$W_{\rm max} = E/2 \,. \tag{21}$$

The DCS for large-W collisions of positrons with free electrons at rest is obtained from the Bhabha formula [10],

$$\frac{{\rm d}\sigma_{\rm Bhabha}}{{\rm d}W} = \frac{2\pi e^4}{m_e v^2} \frac{1}{W^2} \, F_{\rm Bhabha}(W) \,, \tag{22}$$

where

$$F_{\rm Bhabha}(W) = 1 - b_1 \frac{W}{E} + b_2 \left(\frac{W}{E}\right)^2 - b_3 \left(\frac{W}{E}\right)^3 + b_4 \left(\frac{W}{E}\right)^4 \,, \tag{23}$$

with

$$b_1 = \left(\frac{\gamma-1}{\gamma}\right)^2 \frac{2(\gamma+1)^2 - 1}{\gamma^2 - 1} \,,$$

$$b_2 = \left(\frac{\gamma-1}{\gamma}\right)^2 \frac{3(\gamma+1)^2 + 1}{(\gamma+1)^2} \,,$$

$$b_3 = \left(\frac{\gamma-1}{\gamma}\right)^2 \frac{2\gamma(\gamma-1)}{(\gamma+1)^2} \,,$$

$$b_4 = \left(\frac{\gamma-1}{\gamma}\right)^2 \frac{(\gamma-1)^2}{(\gamma+1)^2} \,. \tag{24}$$

2.2. Asymptotic formula for the stopping cross section

When the kinetic energy of the projectile is sufficiently high, the stopping cross section of atoms obtained from the PWBA can be expressed as [13,14]

$$\sigma_{\rm in,asympt}^{(1)} = \frac{2\pi Z_1^2 e^4}{m_e v^2} 2Z \left\{ \ln\left(\frac{2m_e v^2}{I}\right) + \ln\gamma^2 - \beta^2 + \frac{1}{2} f(\gamma) + \frac{S_0 - Z}{2Z} \left[\ln(\beta^2\gamma^2) - \beta^2 \right] \right\} \tag{25}$$

with

$$S_0 = \int_0^{\infty} \frac{{\rm d}f(W)}{{\rm d}W} \, {\rm d}W \,. \tag{26}$$

The quantity I, the mean excitation energy, is defined by

$$\ln\left(\frac{2m_e c^2}{I}\right) = \frac{S_0}{Z} \ln\left(\frac{2m_e c^2}{I_0}\right) + \frac{D_0}{2Z} \tag{27}$$

where

$$\ln I_0 = \frac{1}{S_0}\int_0^\infty \ln W \,\frac{\mathrm{d}f(W)}{\mathrm{d}W}\,\mathrm{d}W \tag{28}$$

and D_0 is an integral of the longitudinal GOS with numerical values of the order of $0.05\,Z$. In the conventional theory [1], which differs from the present approach in that it neglects small relativistic corrections, the I value is defined by the right-hand side of Eq. (28).

The function $f(\gamma)$ has different forms for projectile electrons, positrons, and heavier particles. Explicitly [3,4,14],

$$f(\gamma) = \ln(R) + \left(\frac{m_\mathrm{e}}{M_1}\,\frac{\gamma^2-1}{\gamma}\,R\right)^2, \qquad R = \left[1+\left(\frac{m_\mathrm{e}}{M_1}\right)^2 + 2\gamma\,\frac{m_\mathrm{e}}{M_1}\right]^{-1} \tag{29a}$$

for particles much heavier than the electron,

$$f(\gamma) = \frac{2\gamma^2-1}{\gamma^2} + \frac{1}{8}\left(\frac{\gamma-1}{\gamma}\right)^2 - \left[4-\left(\frac{\gamma-1}{\gamma}\right)^2\right]\ln 2 - \ln(\gamma+1) \tag{29b}$$

for electrons, and

$$f(\gamma) = \frac{\gamma^2-1}{12\gamma^2}\left(1-\frac{14}{\gamma+1}-\frac{10}{(\gamma+1)^2}-\frac{4}{(\gamma+1)^3}\right) - \ln 2 - \ln(\gamma+1) \tag{29c}$$

for positrons.

2.3. Shell correction

The formula (25) approximates the calculated atomic stopping cross section $\sigma_\mathrm{in}^{(1)}$ asymptotically, *i.e.*, when the kinetic energy of the projectile is sufficiently high. The difference $\sigma_\mathrm{in,asympt}^{(1)} - \sigma_\mathrm{in}^{(1)}$ determines the so-called shell correction C/Z, defined so that the corrected formula

$$\sigma_\mathrm{in}^{(1)} = \frac{2\pi\,Z_1^2 e^4}{m_\mathrm{e}v^2}\,2Z\left\{\ln\left(\frac{2m_\mathrm{e}v^2}{I}\right) + \ln\gamma^2 - \beta^2 + \frac{1}{2}\,f(\gamma) - \frac{C(\gamma)}{Z}\right\} \tag{30}$$

reproduces the calculated values of the atomic stopping cross section.

The "modified" shell correction

$$\frac{C'(\gamma)}{Z} \equiv \frac{C(\gamma)}{Z} - \frac{S_0 - Z}{2Z}\left[\ln(\beta^2\gamma^2) - \beta^2\right] \tag{31}$$

for protons has been computed by Salvat et al. [13] for the elements with $Z = 1$ to 99. Because the difference $\sigma_\mathrm{in,asympt}^{(1)} - \sigma_\mathrm{in}^{(1)}$ magnifies numerical inaccuracies of the calculated $\sigma_\mathrm{in}^{(1)}$, the numerical value of $C'(\gamma)/Z$ becomes uncertain for high-energy projectiles. To avoid the influence of those inaccuracies, for projectile protons with energies higher than $E_\mathrm{c} = \min\{0.2Z, 5\}$ MeV, the calculated "modified" shell correction was replaced with the analytical form

$$\frac{C'(\gamma)}{Z} = \sum_{n=1}^{6} p_n(\gamma-1)^n \tag{32}$$

with the parameters p_n ($n = 1$ to 6) determined by a least-squares fit to the numerical values in the energy interval from E_c to 10 GeV. At higher energies, owing to numerical inaccuracies, the value of the modified shell correction is uncertain; for $\gamma > 2$, $C'(\gamma)/Z$ is assumed to be constant and equal to $C'(2)/Z$. As discussed by Salvat [8], these modified shell corrections are valid also for any charged projectile heavier than the electron.

For completeness, we have also determined modified shell corrections for electrons and positrons from the difference $\sigma_\mathrm{in,asympt}^{(1)} - \sigma_\mathrm{in}^{(1)}$, where the numerical stopping cross section $\sigma_\mathrm{in}^{(1)}$ was calculated with the appropriate exchange corrections (see [14]). For electrons and positrons, the parameters of the expression (32) were obtained by fitting the calculated values for energies higher than $E_\mathrm{c} = \min\{Z, 10\}$ keV up to about 1 MeV. The modified shell correction is assumed to be constant for $\gamma > 2$.

The modified shell corrections $C'(\gamma)/Z$ for projectile electrons, positrons, and heavier particles are listed in the database files `eshcor-zz.tab`, `pshcor- zz.tab`, and `shcor-zz.tab`, respectively. The string `zz` in the file names, two digits, denotes the atomic number of the element.

3. Corrected Bethe formula for the electronic stopping power

In a recent study, Salvat [8] has shown that the electronic stopping power of a condensed material for charged projectiles with sufficiently high energy can be calculated from the corrected Bethe formula

$$S_\mathrm{in}(E) = \frac{4\pi\,Z_1^2 e^4}{m_\mathrm{e}v^2}\,\mathcal{N}Z\left\{\ln\left(\frac{2m_\mathrm{e}v^2}{I}\right) + \ln\gamma^2 - \beta^2 + \frac{1}{2}\,f(\gamma) - \frac{C(\gamma)}{Z} - \frac{1}{2}\,\delta_\mathrm{F} + \Delta L^\mathrm{LS} + \Delta L^\mathrm{B}(a)\right\}, \tag{33}$$

where the last three terms are the density-effect correction, the Lindhard–Sørensen correction and the Barkas correction, respectively. The last two corrections are derived under the assumption that the velocity of the projectile changes slowly along its path, which does not hold for electrons and positrons because these particles may change their energy and/or direction of motion appreciably in a single collision. Hence, the Lindhard–Sørensen and Barkas corrections will be excluded in calculations for projectile electrons and positrons.

The mean excitation energy I [see Eqs. (27) and (28)] and the corrections δ_F and $\Delta L^\mathrm{B}(a)$ are determined by the OOS of the material. In the present approach, I is considered as an empirical parameter, which is used to build the OOS model of the material and, consequently, determines its stopping properties.

3.1. DHFS model of the optical oscillator strength

The OOS of the material is modeled as proposed in Ref. [8], from information in the database of atomic subshell GOSs calculated with the DHFS potential [14]. Let $F_i^\mathrm{ion}(Z;W)$ denote the calculated OOS for transitions of individual electrons in the i-th subshell of the atom to final orbitals with positive energy (ionization). To correct for the small discrepancies between subshell ionization energies U_i obtained from the DHFS potential and the experimental ionization energies, the subshell OOS is shifted in energy to the correct (empirical) ionization energies given by Carlson [15]. Excitations to bound atomic levels (a series of discrete resonances with energies below U_i) must be taken into account to preserve the dipole sum rule,

$$\int_0^\infty \frac{\mathrm{d}f(W)}{\mathrm{d}W}\,\mathrm{d}W = Z, \tag{34}$$

which holds exactly in the non-relativistic theory; notice that we are neglecting the small relativistic correction $\Delta(Q=0)$ [cf. Eq. (11)]. Since the details of the excitation spectrum are not important, the contribution of discrete excitations to the OOS are represented approximately by extending the ionization OOS to excitation energies below the ionization threshold. The OOS of the i-th electron subshell is described as

$$F_i(Z;W) = \begin{cases} F_i^{\rm ion}(Z;W) & \text{if } U_i \le W, \\ F_i^{\rm ion}(Z;U_i) & \text{if } U_i' \le W < U_i, \\ 0 & \text{if } W < U_i', \end{cases} \tag{35}$$

with the cutoff energy U_i' such that the product $(U_i - U_i')F_a^{\rm ion}(Z;U_i)$ equals the sum of OOSs for excitations to discrete levels. For the outmost subshells the cutoff energy so defined may be less than $0.5U_i$; in this case, the recipe (34) is modified by setting $U_i' \simeq 0.5U_i$, and defining the constant OOS in the interval (U_i', U_i) so that the subshell contribution to the dipole sum is preserved. The atomic subshell OOSs of the elements are listed in the database files `oos-zz.tab`, where `zz` denotes the atomic number.

The OOS of a monoatomic gas of the element with atomic number Z is approximated as

$$F_{\rm atom}(Z;W) = \sum\nolimits_i F_i(Z;W)\,, \tag{36}$$

where the summation runs over the various electron subshells of the atom in its ground-state configuration. As this atomic OOS may deviate slightly from the dipole sum rule, which is instrumental in the derivation of the Bethe stopping power formula (see, *e.g.*, [1,13]), the OOS is renormalized to fulfill that sum rule. In addition, we shall rescale the excitation energies so as to reproduce the empirical value of the mean excitation energy I through its conventional definition [1], Eq. (28). That is, we express the atomic OOS as

$$\frac{{\rm d}f(Z;W)}{{\rm d}W} = a_1 a_2 F_{\rm atom}(Z; a_2\,W) \tag{37}$$

with the constants a_1 and a_2 determined from the conditions

$$Z = \int_0^\infty \frac{{\rm d}f(Z;W)}{{\rm d}W}\,{\rm d}W = a_1 \int_0^\infty F_{\rm atom}(Z;W')\,{\rm d}W', \tag{38a}$$

where $W' = a_2 W$, and

$$\begin{aligned} \ln I &= \frac{1}{Z}\int_0^\infty \ln W\,\frac{{\rm d}f(Z;W)}{{\rm d}W}\,{\rm d}W \\ &= \frac{1}{Z}\,a_1 \int_0^\infty \ln(W'/a_2)\,F_{\rm atom}(Z;W')\,{\rm d}W' \\ &= -\ln a_2 + \frac{a_1}{Z}\int_0^\infty \ln W'\,F_{\rm atom}(Z;W')\,{\rm d}W'. \end{aligned} \tag{38b}$$

The recipe given by Eqs. (36) and (37) is not suited for compounds and condensed materials, because the wave functions of electrons in outer subshells are strongly affected by atomic aggregation, and the presence of neighboring atoms modifies the final-state orbitals of the active electron [16]. The contributions from inner subshells with binding energies U_i larger than a certain threshold value $W_{\rm th}$ of the order of 50 eV, are relatively insensitive to aggregation and may be approximated by the free-atom form (36). The OOS of electrons in outer subshells with binding energies $U_i < W_{\rm th}$ is represented as the OOS of a single classical damped oscillator with resonance energy $W_{\rm r}$, damping constant Γ, and an energy gap $W_{\rm g}$ in the case of insulators and semiconductors. That is,

$$\begin{aligned} F_{\rm out}(W) = C_{\rm out}\,&\frac{W\sqrt{W^2 - W_{\rm g}^2}}{\left(W_{\rm r}^2 + W_{\rm g}^2 - W^2\right)^2 + \Gamma^2(W^2 - W_{\rm g}^2)} \\ &\times \Theta(W - W_{\rm g})\,\Theta(U_{\rm K,max} - W), \end{aligned} \tag{39}$$

where $C_{\rm out}$ is a normalization constant and $\Theta(x)$ is the Heaviside step function ($=1$ if $x>0$, and $=0$ otherwise). The OOS of the oscillator is truncated at the largest binding energy $U_{\rm K,max}$ of the K shells of the elements present to prevent a tail that would dominate over the atomic OOSs at very large W's. The model OOS is obtained as

$$\frac{{\rm d}f(W)}{{\rm d}W} = F_{\rm out}(W) + \sum\nolimits_i F_i(Z;W)\,\Theta(W - W_{\rm th}), \tag{40}$$

where the summation runs over the inner subshells, whose OOSs are truncated at $W_{\rm th}$. The constant $C_{\rm out}$ is determined by requiring that the dipole sum rule (34) is satisfied, *i.e.*,

$$\begin{aligned} \int_{W_{\rm g}}^{U_{\rm K,max}} F_{\rm out}(W)\,{\rm d}W &= Z - \int_{W_{\rm th}}^{\infty} \left(\sum\nolimits_i F_i(Z;W)\right){\rm d}W \\ &= f_{\rm out}, \end{aligned} \tag{41}$$

and the resonance energy $W_{\rm r}$ is set equal to the plasma resonance energy of an electron gas with the average density of electrons in outer subshells (including contributions from truncated inner subshells),

$$W_{\rm r} = \sqrt{4\pi\mathcal{N} f_{\rm out}\frac{\hbar^2 e^2}{m_{\rm e}}}, \tag{42}$$

where $\hbar$ is the reduced Planck constant. The gap energy $W_{\rm g}$ is null for conductors, and should be determined from knowledge of experimental information (*e.g.*, from Refs. [17–19]) in the case of semiconductors and insulators. Finally the damping constant Γ is fixed by requiring that the OOS yields the empirical I value of the material, as given, *e.g.*, in the ICRU Report 37 [3]. The OOS build in this way has a realistic appearance for large energy transfers W, it satisfies the dipole sum rule, and it yields the adopted empirical I value.

3.2. Density-effect correction

This correction, which was first studied by Fermi [20], accounts for the effect of the dielectric polarization of the medium, which makes the stopping power of a dense material smaller than that of a thin gas of the same composition. The density-effect correction is calculated from the formula derived by Fano [21] for high-energy projectiles, which is equivalent to (see Ref. [22])

$$\delta_{\rm F} \equiv \frac{1}{Z}\int_0^\infty \frac{{\rm d}f(W)}{{\rm d}W}\ln\left(1 + \frac{L^2}{W^2}\right){\rm d}W - \frac{L^2}{\Omega_{\rm p}^2}\left(1 - \beta^2\right), \tag{43}$$

where L is the positive root of the equation

$$\mathcal{F}(L) \equiv \frac{1}{Z}\Omega_{\rm p}^2 \int_0^\infty \frac{1}{W^2 + L^2}\frac{{\rm d}f(W)}{{\rm d}W}\,{\rm d}W = 1 - \beta^2. \tag{44}$$

The quantity

$$\Omega_{\rm p} = \sqrt{4\pi\,\mathcal{N}Z\,\frac{\hbar^2 e^2}{m_{\rm e}}}, \tag{45}$$

is the plasma resonance energy of an electron gas with the average electron density $\mathcal{N}Z$ of the material; $\hbar$ is the reduced Planck constant. The function $\mathcal{F}(L)$ decreases monotonically with L, and hence, the root $L(\beta^2)$ exists only when $1-\beta^2 < \mathcal{F}(0)$; otherwise it is $\delta_{\rm F}=0$. Therefore, the function $L(\beta^2)$ starts with zero at $\beta^2 = 1-\mathcal{F}(0)$ and grows monotonically with increasing β^2.

In the high-energy limit ($\beta\to 1$), the L value resulting from Eq. (44) is large and it can be approximated as $L^2 = \Omega_{\rm p}^2/(1-\beta^2)$. Then, using the dipole sum rule and the relation (38b), we obtain

$$\delta_{\rm F} \simeq \ln\left(\frac{\Omega_{\rm p}^2}{(1-\beta^2)I^2}\right) - 1 \qquad \text{when } \beta\to 1. \tag{46}$$

Therefore, because of the density-effect correction the electronic stopping power of high-energy projectiles is determined by the electron density of the material, *i.e.*, it is independent of the I value.

As the density-effect correction $\delta_{\rm F}$ is significant only for projectiles with high energies, the value obtained from the formula (43) can also be used when the energy of the projectile is low or moderate.

3.3. Lindhard–Sørensen correction

This correction accounts for the differences between the exact DCS for collisions of the projectile with electrons [23] and its perturbative approximation to first order. In the non-relativistic limit, it reduces to the Bloch correction, which is given by

$$Z_1^2 L_2^{\rm Bloch} = -\eta^2 \sum_{n=1}^{\infty} \frac{1}{n(n^2+\eta^2)}\,, \tag{47}$$

where

$$\eta = \frac{Z_1 e^2}{\hbar v} \tag{48}$$

is the Sommerfeld parameter.

For pointlike projectiles with small charges ($|Z_1|\leq 2$) and energies less than $10^2 M_1 c^2$, the Lindhard–Sørensen correction calculated numerically is closely approximated by the following analytical expression [8]

$$\Delta L_{\rm point}^{\rm LS} = \left(\frac{1+A}{1+1.92\,(\gamma-1)^{1.41}} - A\right) Z_1^2 L_2^{\rm Bloch}, \tag{49}$$

where $A=180.20$ for $Z_1=+1$ (protons, deuterons, tritons, antimuons), $A=-178.34$ for $Z_1=-1$ (antiprotons, muons), $A=90.59$ for $Z_1=+2$ (alphas), and $A=-88.73$ for $Z_1=-2$. Values from this empirical formula differ from accurate numerical results for pointlike projectiles with $Z_1=\pm 1$ and ± 2 in less than about 5×10^{-4}.

3.4. Barkas correction

In the classical derivation by Bohr [24] of a formula for the electronic stopping power, the contribution from distant interactions is evaluated by assuming that electrons behave as classical oscillators under the action of the electric field of the projectile, which is assumed to be constant over the atomic volume. The Barkas correction accounts for the (linear) variation of that electric field over the volume swept by the target electron. This correction is evaluated as [25,26]

$$\Delta L^{\rm B}(a) = \frac{Z_1\alpha}{\gamma^2\beta^3 m_{\rm e}c^2}\,\frac{1}{Z}\int_0^{W_{\rm max}} {\rm d}W\,\frac{{\rm d}f(W)}{{\rm d}W} \times W\left[I_1(\xi) + \frac{1}{\gamma^2}\,I_2(\xi)\right], \tag{50}$$

with $\xi = Wa/(\gamma v\hbar)$, where a is a cutoff impact parameter that separates close and distant interactions, which for elemental materials is estimated as [8]

$$a = C_{\rm B}\,0.5616\,\frac{\hbar}{m_{\rm e}v}\,, \tag{51}$$

with $C_{\rm B} = \max\{1, Z/10\}$. The functions $I_1(\xi)$ and $I_2(\xi)$ are defined by triple integrals involving modified Bessel functions of orders 0 and 1 [25,26], which were calculated numerically. To facilitate further calculations, these functions have been fitted by analytical expressions in various subintervals that approximate the numerical results with an accuracy better than 0.1% for ξ from 0 to ∼15. The adopted parameterizations of $I_1(\xi)$ and $I_2(\xi)$ can be found in the source file `sbethe.f` of the program, functions `ARBI1(X)` and `ARBI2(X)`.

3.5. Corrected Bethe formula for compound materials

The corrected Bethe formula (33) is applicable to arbitrary materials, including compounds and mixtures of various elements. Let us consider a compound whose molecules consist of n_j atoms of the element of atomic number Z_j. The mean excitation energy of the compound can be estimated by using the additivity approximation, *i.e.*, by assuming that the molecular cross section can be approximated as the sum of atomic cross sections of the atoms in a molecule. The OOS of a molecule is then the sum of the OOSs of its atoms and, consequently, the I value of the compound is given by

$$Z\ln I = \sum\nolimits_j n_j Z_j \ln(I_j) \quad \text{with} \quad Z = \sum\nolimits_j n_j Z_j\,, \tag{52}$$

where I_j denotes the mean excitation energy of the element with atomic number Z_j. Since the additivity approximation neglects the effect of aggregation on the atomic OOSs, the I value resulting from Eq. (52) may differ appreciably from the "true" mean excitation energy of the material. A better estimate of the I value can only be obtained either from stopping measurements or from knowledge of the OOS of the material.

As discussed by Salvat [8], the atomic shell correction obtained from the PWBA is valid for arbitrary materials, because the main contribution to that correction arises from inner electron subshells, which are only slightly affected by aggregation effects. The shell correction $C(\gamma)/Z$ of the compound, obtained from the additivity approximation, is given by

$$\frac{C(\gamma)}{Z} = \frac{1}{Z}\sum_j Z_j\,\frac{C_j(\gamma)}{Z_j}, \tag{53}$$

where the quantity $C_j(\gamma)/Z_j$ is the shell correction for the elemental material of atomic number Z_j. The cutoff impact parameter a, which determines the Barkas correction, may be estimated from Eq. (51) with

$$C_{\rm B} = \max\{1, \overline{Z}/10\} \quad \text{where} \quad \overline{Z} = Z\left(\sum\nolimits_j n_j\right)^{-1}. \tag{54}$$

As indicated above, the electronic stopping power obtained from the corrected Bethe formula is completely determined by the adopted value of the mean excitation energy I. By default, the program SBETHE sets $I = I_{\rm ICRU}$, the I value recommended in the Report 37 of the ICRU [3], which yields results in close agreement with available experimental stopping powers [8]. In order to allow analyzing the dependence of the calculated stopping power on this parameter, the user is allowed to modify its default value.

3.6. Electron capture by positively charged ions

A fundamental assumption of the PWBA is that the projectile behaves as a traveling point particle with constant charge. This is not true for slow positive ions, which capture electrons from the medium and loose them through a complex dynamical process. Experimental evidence gives support to Bohr's suggestion that the orbital velocity of bound electrons is the dominant parameter of the process, and that an ion gets stripped of all its electrons that (in their bound orbitals) have orbital velocities smaller than the velocity of the ion (see Ref. [2] and references therein). In the case of light ions with small charges ($Z_1 \leq 2$), it is natural to consider that the capture process is ruled by the velocity of an electron bound to the ion in the ground state, which may be estimated from the hydrogenic model as $c\alpha Z_1$, where $\alpha \simeq 1/137$ is the fine structure constant. To account for electron capture effects, for protons and alphas the SBETHE program replaces the factor Z_1 in Eq. (33) with the effective charge of the ion, estimated by means of the empirical formula

$$Z_1^* = Z_1 \left[1 - \exp\left(\frac{-\beta}{\alpha Z_1}\right)\right], \tag{55}$$

which is analogous to the usual expression for heavy ions, with the velocity of captured electrons evaluated from the hydrogenic model rather than from the Thomas–Fermi model.

3.7. Low-energy extrapolation

The results from the corrected Bethe formula, calculated from the present approach, closely approximate the measured stopping powers for protons and alpha particles with kinetic energies higher than a value $E_{\rm cut}$ of the order of 0.75 MeV and 5 MeV respectively. The very limited experimental information available on the stopping of low energy electrons, suggests that the formula is also valid for electrons, and positrons, with kinetic energies higher than $E_{\rm cut} \sim 1$ keV. In order to permit the approximate calculation of particle ranges of low-energy projectiles [see Eq. (71) below], it is convenient to extrapolate the predictions of the Bethe formula to energies lower than $E_{\rm cut}$. Our aim here is not to give reliable stopping powers for low-energy projectiles, but simply to permit estimating the order of magnitude of their ranges.

Inspection of available experimental data for protons and alphas [8] indicates that the stopping power of these particles has a wide maximum at an energy $E_{\rm max}$ of about 50 keV for protons and 0.8 MeV for alphas [8]. The stopping power for electrons has a similar energy dependence, with a maximum at $E_{\rm max} \sim 100$ eV.

The program SBETHE calculates the electronic stopping power from the corrected Bethe formula (33) for energies higher than $E_{\rm cut}$, which the program sets equal to 1 keV for electrons and positrons, 150 keV for muons and antimuons, 0.75 MeV for protons and antiprotons, and 5 MeV for alpha particles. The calculated values are extrapolated to lower energies by using the analytical form

$$S_{\rm in}(E) = \begin{cases} \exp\left[A - B\,(\ln t)^{1.5}\right] & \text{if } E_{\rm max} \leq E \leq E_{\rm cut}, \\ 1.5\,\exp(A)\,\sqrt{t}\left(1 - \dfrac{t}{3}\right) & \text{if } E \leq E_{\rm max}, \end{cases} \tag{56}$$

with $t = E/E_{\rm max}$, and the parameters A and B determined by requiring continuity of $S_{\rm in}(E)$ and its derivative at $E = E_{\rm cut}$. The energy dependence at low energies, $S_{\rm in} \propto \sqrt{E}$, is in accordance with the theory of the free-electron gas (which predicts that the stopping power of slow projectiles is proportional to their velocity [27]).

Electronic stopping cross sections of noble gases for protons and alpha particles calculated with the SBETHE program are compared with results from measurements in Fig. 1. The experimental data were taken from the exhaustive IAEA online database[1] on "Electronic Stopping Power of Matter for Ions" [28]. The vertical lines are at the energy $E_{\rm cut}$ above which the corrected Bethe formula is applied. Below this energy, the plotted values were generated from the extrapolation formula (56). In spite of the simplicity of that formula, its results follow the global trends of the experimental data.

Fig. 2 compares stopping powers of metallic aluminum, silicon, copper, and gold for projectile electrons calculated by the SBETHE program with experimental data from the Refs. [29–33]. The dashed portion of the curves are results from the extrapolation (56), which yields realistic values of the electronic stopping power for electron energies down to about 100 eV.

4. Radiative stopping power for electrons and positrons

Electrons and positrons, because of their small mass, experience large accelerations when they penetrate the electrostatic field of an atom, or of an electron, and, as a result, they emit bremsstrahlung (braking radiation). A thorough review of the theory and experimental measurements of bremsstrahlung emission is given in the monograph by Haug and Nakel [34]. The process is responsible for the radiative stopping power, which dominates the stopping power for high-energy electrons and positrons.

In each bremsstrahlung event, an electron with kinetic energy E emits a photon of energy W, which may take values in the interval from 0 to E. The relevant information on the radiative process is provided by the atomic energy-loss DCS, differential in only the energy W of the emitted photon (see [3] and references therein). Theoretical considerations [35,36] show that the DCS for bremsstrahlung emission in the field of an atom of atomic number Z can be expressed in the form

$$\frac{{\rm d}\sigma_{\rm rad}}{{\rm d}W} = \frac{Z^2}{\beta^2}\,\frac{1}{W}\,\chi(Z, E; \kappa), \tag{57}$$

where κ is the reduced photon energy,

$$\kappa \equiv W/E, \tag{58}$$

which takes values between 0 and 1. The quantity

$$\chi(Z, E; \kappa) \equiv (\beta^2/Z^2) W \frac{{\rm d}\sigma_{\rm rad}}{{\rm d}W} \tag{59}$$

is known as the "scaled" bremsstrahlung DCS; for atoms of a given element Z, it varies smoothly with E and κ. Seltzer and Berger [6,7] produced extensive tables of the scaled DCS for all the elements (Z =1–99) and for electron energies from 1 keV to 10 GeV. They tabulated the scaled DCSs for emission in the (screened) field

[1] This database is available from the IAEA web site, https://www-nds.iaea.org/stopping/index.html. Data downloaded in March 2022.

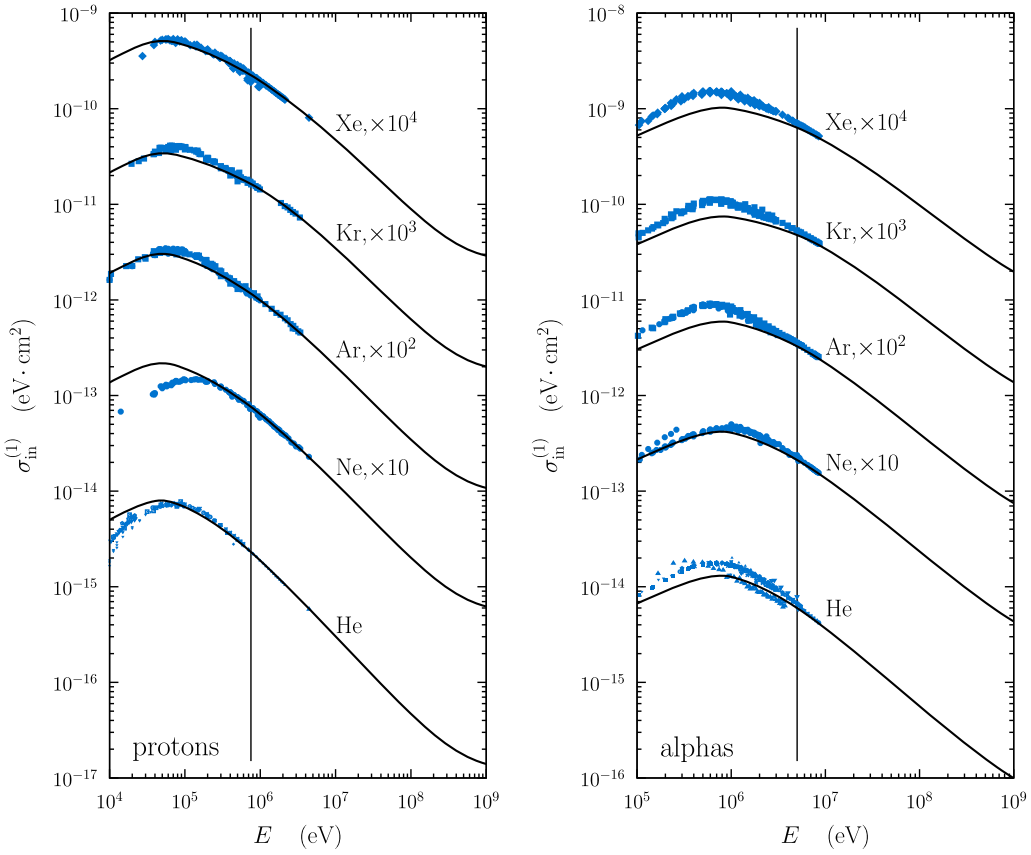

Fig. 1. Electronic stopping cross sections of noble gases for protons (left) and alpha particles (right) as functions of the kinetic energy of the projectile, multiplied by the indicated powers of 10 to improve visibility. Solid curves are results from SBETHE. Symbols represent experimental data from the IAEA database. Other details are explained in the text.

of the nucleus (electron-nucleus bremsstrahlung) and in the field of atomic electrons (electron-electron bremsstrahlung) separately, as well as their sum, the total scaled DCS. The electron-nucleus bremsstrahlung DCS was calculated by combining analytical high-energy theories with results from partial-wave calculations by Pratt et al. [37,38] for bremsstrahlung emission in screened atomic fields and energies below 2 MeV. The scaled DCS for electron-electron bremsstrahlung was obtained from the theory of Haug [39] combined with a screening correction that involves Hartree–Fock incoherent scattering functions. Seltzer and Berger's scaled DCS tables constitute the most reliable theoretical representation of bremsstrahlung energy spectra available at present.

The total atomic cross section for bremsstrahlung emission is infinite due to the divergence of the DCS (57) at $W = 0$ (the so-called infrared divergence), which is associated with the null mass of the photon. Nevertheless, the radiative stopping cross section,

$$\sigma_{\rm rad}^{(1)}(E) \equiv \int_0^E W \frac{{\rm d}\sigma_{\rm rad}}{{\rm d}W}\,{\rm d}W = \frac{Z^2}{\beta^2} E \int_0^1 \chi(Z, E; \kappa)\,{\rm d}\kappa\,, \tag{60}$$

is finite. The radiative stopping power (*i.e.*, the average energy radiated per unit path length) is

$$S_{\rm rad}(E) = \mathcal{N}\sigma_{\rm rad}^{(1)}(E), \tag{61}$$

where $\mathcal{N}$ is the number of atoms per unit volume. The tables of Seltzer and Berger include the quantity

$$\phi_{\rm rad}(Z, E) \equiv \frac{1}{Z^2 \alpha r_{\rm e}^2 (E + m_{\rm e}c^2)} \int_0^E W \frac{{\rm d}\sigma_{\rm rad}}{{\rm d}W}\,{\rm d}W\,, \tag{62}$$

where α is the fine-structure constant and $r_{\rm e} = \alpha^2 a_0$ is the classical electron radius. The stopping power of elemental materials for electrons with kinetic energy E can then be calculated easily by interpolation of the Seltzer and Berger tables.

In the case of compounds (or mixtures), the molecular DCS is obtained from the additivity approximation, *i.e.*, as the sum of the DCSs of all the atoms in a molecule. Consider a compound whose molecules consist of n_j atoms of the element Z_j. The molecular DCS is

$$\frac{{\rm d}\sigma_{\rm rad,mol}}{{\rm d}W} = \frac{1}{\beta^2 W} \sum_j n_j Z_j^2\, \chi(Z_j, E; \kappa). \tag{63}$$

The radiative stopping power of the compound is

$$S_{\rm rad}(E) = \mathcal{N}\alpha r_{\rm e}^2 (E + m_{\rm e}c^2) \sum_j n_j Z_j^2\, \phi_{\rm rad}(Z_j, E), \tag{64}$$

where $\mathcal{N}$ is the number of molecules per unit volume.

The radiative DCS and the stopping power for positrons are generally smaller than those for electrons because positrons are repelled by the nucleus and, therefore, experience less acceleration than electrons with the same energy. Owing to the lack of more detailed calculations, the atomic DCS for positrons is obtained by multiplying the electron DCS by a κ-independent factor, *i.e.*,

$$\frac{{\rm d}\sigma_{\rm rad}^{(+)}}{{\rm d}W} = F_{\rm p}(Z, E)\, \frac{{\rm d}\sigma_{\rm rad}^{(-)}}{{\rm d}W}. \tag{65}$$

The factor $F_{\rm p}(Z, E)$ is set equal to the ratio of the radiative stopping powers for positrons and electrons, which has been calculated

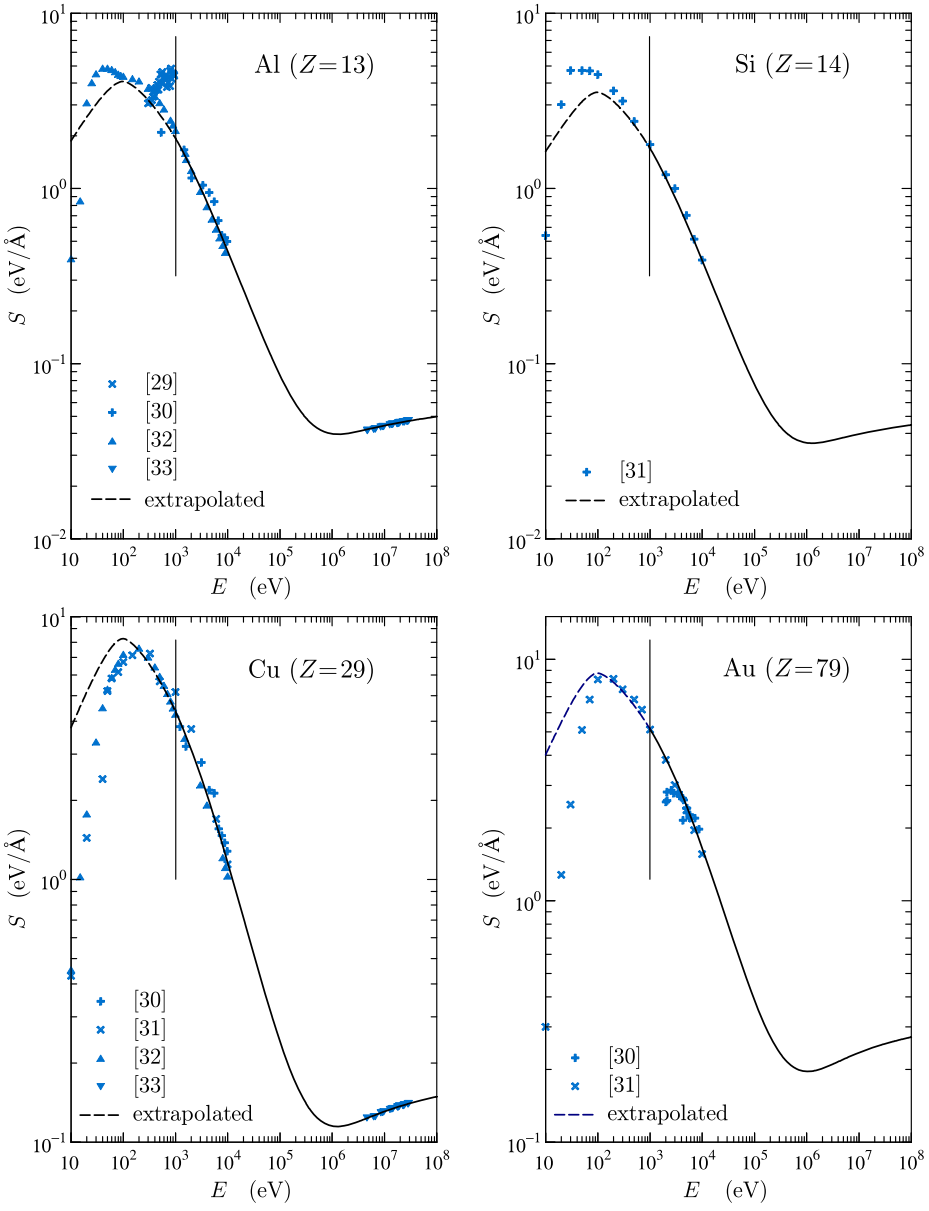

Fig. 2. Electronic stopping powers of solid aluminum, silicon, copper, and gold for electrons, as functions of the kinetic energy E. The curves are results from SBETHE. Symbols represent experimental data from the indicated references.

by Kim et al. [40,41]. In the calculations we use the following analytical approximation

$$F_{\rm p}(Z,E) = 1 - \exp(-1.2359\times10^{-1}\,t + 6.1274\times10^{-2}\,t^2 - 3.1516\times10^{-2}\,t^3 + 7.7446\times10^{-3}\,t^4 - 1.0595\times10^{-3}\,t^5 + 7.0568\times10^{-5}\,t^6 - 1.8080\times10^{-6}\,t^7), \quad (66)$$

where

$$t = \ln\left(1 + \frac{10^6}{Z^2}\frac{E}{m_{\rm e}c^2}\right). \quad (67)$$

Expression (66) reproduces the values of $F_{\rm p}(Z,E)$ tabulated by Kim et al. [40] to an accuracy of about 0.5%. Correspondingly, the radiative stopping power of a compound material for positrons is calculated as

$$S^{(+)}_{\rm rad}(E) = \mathcal{N}\alpha r_{\rm e}^2 (E + m_{\rm e}c^2) \sum_j n_j Z_j^2\, F_{\rm p}(Z_j,E)\,\phi_{\rm rad}(Z_j,E). \quad (68)$$

Fig. 3 compares the radiative mass stopping powers of electrons in solid aluminum, silver, and gold, with the corresponding electronic stopping powers. The total stopping power

$$S(E) = S_{\rm in}(E) + S_{\rm rad}(E), \quad (69)$$

determines the projectile range [see Eq. (71)]. While electronic stopping dominates at low energies, it is outweighed by radiative stopping at high energies.

5. The program SBETHE

The Fortran program SBETHE calculates the electronic stopping power of a material for fast charged particles from the corrected Bethe formula, Eq. (33), with the various corrections computed as described in the text. The program utilizes a database of subshell OOSs and atomic shell corrections obtained from PWBA calcula-

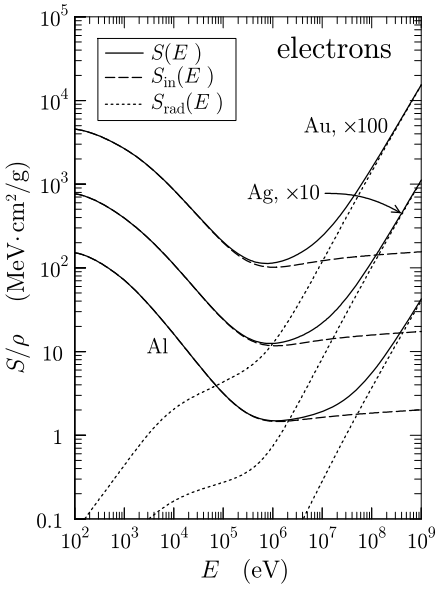

Fig. 3. Electronic, radiative, and total mass stopping powers (dashed, dotted, and solid curves, respectively) for electrons in solid aluminum, silver (×10), and gold (×100) as functions of the kinetic energy of the projectile.

tions with the DHFS self-consistent potential of free neutral atoms [8,12,13].

The Fortran program and the associated database are distributed in a single compressed zip file named `sbethe.zip`. Its contents consists of a single directory named `./sbethe` with two subdirectories.

• The root directory `./sbethe` contains the set of files of the SBETHE code:

1) the Fortran source file `sbethe.f` of the program, and its executable binary file `sbethe.exe` generated with the Intel Fortran compiler on a Windows 10 64-bit platform,

2) three GNUPLOT scripts with the extension `.gnu` for visualizing the calculation results, and

3) the text file `material-list.txt` is the list of 280 materials of radiological interest that are pre-defined in the file `pdcompos.pen`, with their identification numbers. The first 99 materials are the elements ($Z = 1$ to 99), ordered by atomic number. Materials 100 to 280 are compounds and mixtures, in alphabetical order.

• The subdirectory `./docs` includes the preprint of the present article and the document `rpwba.pdf` with details on the PWBA theory and numerical methods used in the calculations of the GOS and integrated cross sections.

• The subdirectory `./sdbase` contains the following 497 ASCII files. The string `zz` in the file names denotes the atomic number of the element, two digits:

◦ 99 files `oos-zz.tab` with tables of the subshell OOSs that were extracted from the database of GOSs calculated with the DHFS potential.

◦ 99 files `shcorr-zz.tab` with tables of the atomic modified shell correction $C'(\gamma)/Z$ (see Section 2.3) for protons and other projectiles heavier then the electron.

◦ 99 files `eshcorr-zz.tab` with tables of the atomic modified shell correction $C'(\gamma)/Z$ for electrons.

◦ 99 files `pshcorr-zz.tab` with tables of the atomic modified shell correction $C'(\gamma)/Z$ for positrons.

◦ 99 files `pdebr-zz.p08` with tables of scaled bremsstrahlung DCSs, $\chi(Z, E; \kappa)$, and integrated cross sections, $\phi_{\rm rad}(Z, E)$, for electrons (Section 4).

◦ `pdatconf.p14`, this file contains a list of ground-state configurations, and subshell ionization energies [15] of free atoms of the elements.

◦ `pdcompos.pen` contains composition data and physical parameters for the materials listed in `material-list.txt`, taken from the database of the ESTAR program of Berger [42].

To run the program on your computer, copy the directory `./sbethe` from the zip file into the hard disc, keeping the structure of its contents unchanged. The binary file `sbethe.exe` will work only under Windows 64-bit operating systems; to obtain the executable file for other platforms, the user must compile the Fortran source file, and replace the Windows executable. Notice that `sbethe.exe` assumes that the database files are in the subdirectory `./sdbase` of its own directory.

The program SBETHE runs interactively, input data are entered from the keyboard following the program prompts, which are self-explanatory. The program starts by asking the name `mname` of the material, an alphanumeric string of up to 15 characters. If a file with the name `mname.mat` exists in the working directory, the program reads the material parameters (composition, mass density and mean excitation energy) and the OOS from that file. Otherwise, SBETHE asks for the parameters of the material, and builds the OOS table by using the DHFS subshell OOSs in the database. To minimize the amount of input information, the program can read the material characteristics from the file `pdcompos.pen`; the list of predefined materials with their identifying numbers is given in the file `material-list.txt`. Once the material parameters and the OOS table are set, the program writes them in the output file `mname.mat`, which will be read directly in future runs for that material. The user can select the kind of projectile particle among the default options (electrons, positrons, negative muons, antimuons, protons, antiprotons, and alphas), or enter the charge and mass of the desired projectile.

The electronic stopping powers obtained from the corrected Bethe formula are determined by the adopted values of the mean excitation energy I. By default, the program sets $I = I_{\rm ICRU}$, the I value recommended in the ICRU Reports 37 and 90 [3,5]. The results shown in Figs. 1 and 2 were generated with this default I value. In order to permit analyzing the dependence of the calculated stopping power on the adopted mean excitation energy, the user is allowed to change the proposed value of this parameter. With the default I value and for projectiles with $E > E_{\rm cut}$, the results from the program are in close agreement with the ICRU recommended stopping powers [3–5].

The SBETHE program generates tables of the stopping power and related quantities for a nearly logarithmic grid of kinetic energies of the projectile with 66 points per decade. The output of SBETHE consists of the following formatted text files:

• `OOS.dat`: optical oscillator strength $F(W) \equiv {\rm d}f(W)/{\rm d}W$ of the material, as a function of the excitation energy W, calculated from the DHFS-model atomic subshell OOSs with the adopted I value, as described in Section 3.1.

• `stplog.dat`: table of the electronic stopping cross section per atom or molecule, $\sigma_{\rm in}^{(1)} \equiv S_{\rm in}/\mathcal{N}$, calculated from the corrected Bethe formula (33), the Bethe "logarithm"

$$L_0 \equiv \ln\left(\frac{2m_{\rm e}v^2}{I}\right) + \ln\gamma^2 - \beta^2, \tag{70}$$

the function $f(\gamma)/2$, and the corrections $C(\gamma)/Z$, $\delta_{\rm F}/2$, $\Delta L^{\rm LS}$ and $\Delta L^{\rm B}(a)$.

• `stp.dat`: table of the electronic stopping power calculated from the corrected Bethe formula, Eq. (33), with and without the shell correction (useful for visualizing the effect of the shell correction).

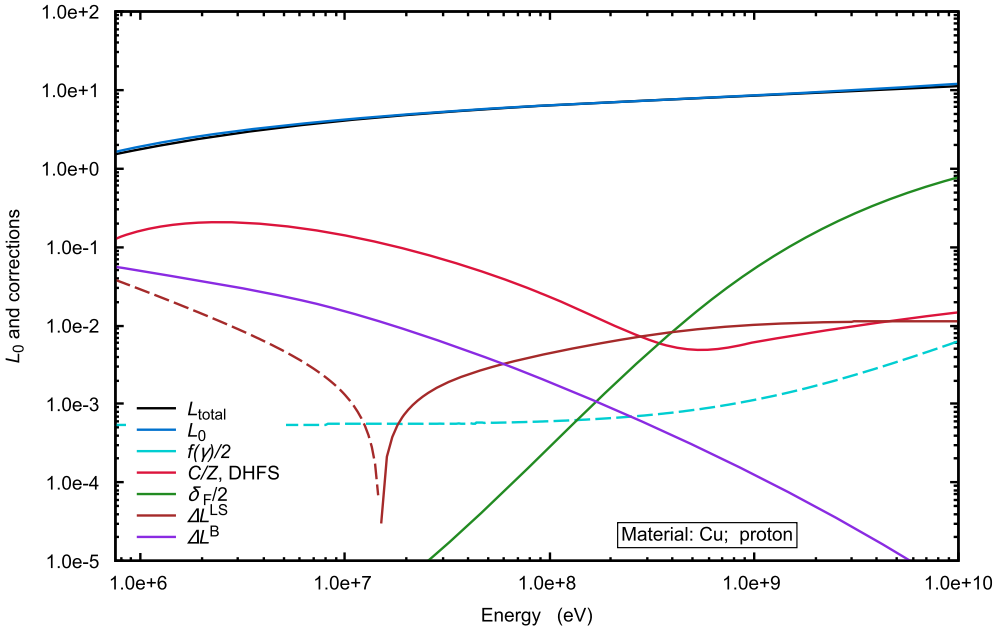

Fig. 4. Results from SBETHE for protons in solid copper, plotted with GNUPLOT by using the provided scripts. Terms in the corrected Bethe formula (33), as functions of the kinetic energy of the projectile.

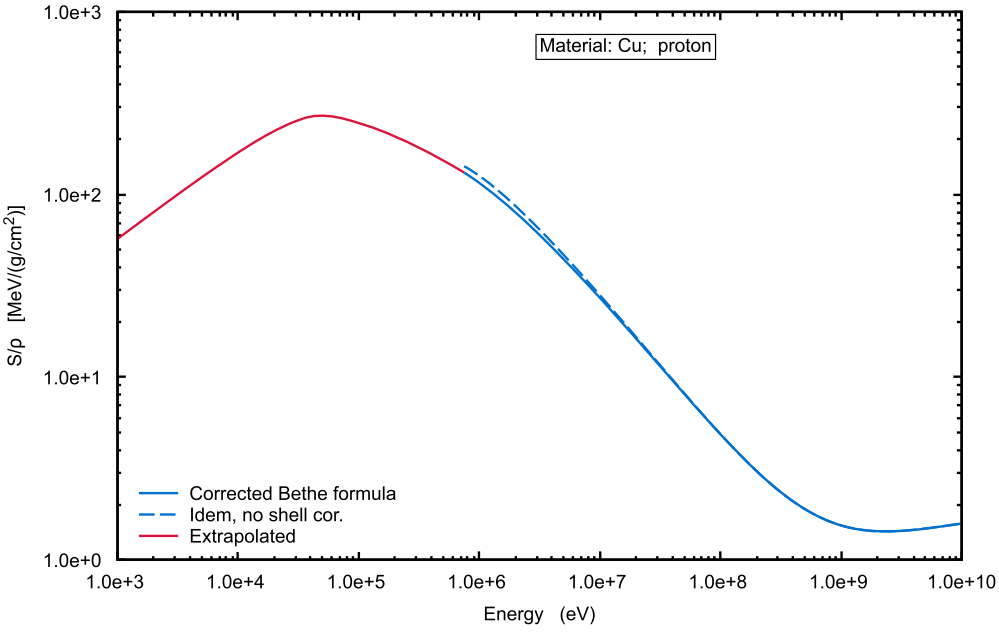

Fig. 5. Results from SBETHE for protons in solid copper, plotted with GNUPLOT by using the provided scripts. Mass stopping power as a function of the kinetic energy of the projectile.

• `stp-low.dat`: table of the electronic stopping power obtained from the low-energy extrapolation, Eq. (56), of results from the corrected Bethe formula.

• `lstp.dat`: tables of the electronic stopping power (including the low-energy extrapolation), the radiative stopping power (null for projectiles heavier than the electron), and their sum, the total stopping power, Eq. (69), all in eV/Å. The fifth column is the CSDA range in cm,

$$R = \int_{E_{abs}}^{E} \frac{\mathrm{d}E}{S(E)}, \tag{71}$$

where E_{abs} is the lowest energy in the table or plot.

• `mstp.dat`: table of the electronic, radiative and total mass stopping powers, $S(E)/\rho$ (in MeV cm^2/g), and the CSDA range times the mass density of the material (in g/cm^2).

The output files are in a format ready for visualization with a plotting program. We recommend using GNUPLOT, which is small in size, available for various platforms (including Linux and Windows) and free; this software package can be downloaded from the distribution sites listed at the GNUPLOT homepage, http://www.gnuplot.info. The output file `gnuinfo.txt` contains information used by these scripts.

Results from SBETHE for projectile protons and electrons in copper (material identification number 29) are displayed in Figs. 4 to 6, which are screen shots of the plots generated with the provided

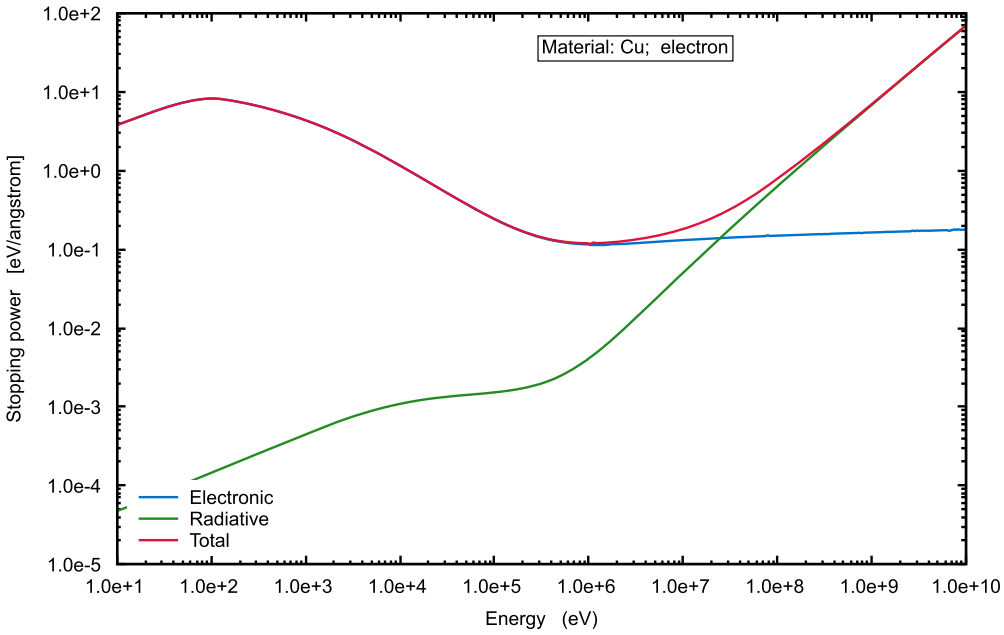

Fig. 6. Results from SBETHE for electrons in solid copper, plotted with GNUPLOT by using the provided scripts. Electron stopping powers as functions of the kinetic energy of the projectile.

GNUPLOT scripts. Of course, these scripts will work only when GNUPLOT is installed on the computer. When the extension ".gnu" is associated to GNUPLOT, a script can be executed by simply clicking the mouse with the pointer on the script icon.

Declaration of competing interest

The authors declare that they have no known competing financial interests or personal relationships that could have appeared to influence the work reported in this paper.

Data availability

No data was used for the research described in the article.

Acknowledgements

Financial support from the Spanish Ministerio de Ciencia e Innovación / Agencia Estatal de Investigación / European Regional Development Fund, European Union, (projects nos. RTI2018-098117-B-C22 and PID2021-123879 OB-C22) is gratefully acknowledged.

References

[1] U. Fano, Annu. Rev. Nucl. Sci. 13 (1963) 1–66.
[2] S.P. Ahlen, Rev. Mod. Phys. 52 (1980) 121–173.
[3] ICRU Report 37, Stopping Powers for Electrons and Positrons, ICRU, Bethesda, MD, 1984.
[4] ICRU Report 49, Stopping Powers and Ranges for Protons and Alpha Particles, ICRU, Bethesda, MD, 1993.
[5] ICRU Report 90, Key Data for Ionizing-Radiation Dosimetry: Measurement Standards and Applications, ICRU, Bethesda, MD, 2016.
[6] S.M. Seltzer, M.J. Berger, Nucl. Instrum. Methods B 12 (1985) 95–134.
[7] S.M. Seltzer, M.J. Berger, At. Data Nucl. Data Tables 35 (1986) 345–418.
[8] F. Salvat, Phys. Rev. A 106 (2022) 032809.
[9] C. Møller, Ann. Phys. 14 (1932) 531–585.
[10] H.J. Bhabha, Proc. Phys. Soc. A 154 (1936) 195–196.
[11] H.A. Bethe, R. Jackiw, Intermediate Quantum Mechanics, Westview Press, Boulder, CO, 1997.
[12] D. Bote, F. Salvat, Phys. Rev. A 77 (2008) 042701.
[13] F. Salvat, L. Barjuan, P. Andreo, Phys. Rev. A 105 (2022) 042813.
[14] F. Salvat, Inelastic collisions of fast charged particles with atoms. Relativistic plane-wave Born approximation, Report Universitat de Barcelona, Barcelona, 2021, unpublished, included in the documentation of the SBETHE program.
[15] T.A. Carlson, Photoelectron and Auger Spectroscopy, Plenum Press, New York, 1975.
[16] J.J. Rehr, R.C. Albers, Rev. Mod. Phys. 72 (2000) 621–654.
[17] E.D. Palik (Ed.), Handbook of Optical Constants of Solids, Academic Press, San Diego, CA, 1985.
[18] E.D. Palik (Ed.), Handbook of Optical Constants of Solids II, Academic Press, San Diego, CA, 1991.
[19] E.D. Palik (Ed.), Handbook of Optical Constants of Solids III, Academic Press, San Diego, CA, 1998.
[20] E. Fermi, Phys. Rev. 57 (1940) 485–493.
[21] U. Fano, Phys. Rev. 103 (1956) 1202–1218.
[22] M. Inokuti, D.Y. Smith, Phys. Rev. 25 (1982) 61–66.
[23] J. Lindhard, A.H. Sørensen, Phys. Rev. A 53 (1996) 2443–2456.
[24] N. Bohr, Philos. Mag. 25 (1913) 10–31.
[25] J. Ashley, R.H. Ritchie, W. Brandt, Phys. Rev. B 5 (1972) 2393–2397.
[26] J.D. Jackson, R.L. McCarthy, Phys. Rev. B 6 (1972) 4131–4141.
[27] J. Lindhard, Dan. Mat. Fys. Medd. 28 (8) (1954) 1–57.
[28] C.C. Montanari, P. Dimitriou, Nucl. Instrum. Methods B 408 (2017) 50–55.
[29] F.W. Garber, M.Y. Nakai, J.A. Harter, R.D. Birkhoff, J. Appl. Phys. 42 (1971) 1149.
[30] K.O. Al-Ahmad, D.E. Watt, J. Phys. D, Appl. Phys. 16 (1983) 2257–2267.
[31] S. Luo, X. Zhang, D.C. Joy, Radiat. Eff. Defects Solids 117 (1991) 235–242.
[32] D.C. Joy, A database of electron-solid interactions, Tech. Rep., University of Tennessee, 2008, unpublished, downloaded from https://studylib.net/.
[33] M.S. MacPherson, Accurate measurements of the collision stopping powers for 5 to 30 MeV electrons, Ph.D. thesis, Carleton University, Ottawa, Ontario, 1998. Also available as document PIRS-0626, National Research Council, Canada.
[34] E. Haug, W. Nakel, The Elementary Process of Bremsstrahlung, World Scientific, Singapore, 2004.
[35] H.A. Bethe, W. Heitler, Proc. R. Soc. A 146 (1934) 83–112.
[36] Y.S. Tsai, Rev. Mod. Phys. 46 (1974) 815–851.
[37] R.H. Pratt, H.K. Tseng, C.M. Lee, L. Kissel, At. Data Nucl. Data Tables 20 (1977) 175–209.
[38] R.H. Pratt, H.K. Tseng, C.M. Lee, L. Kissel, At. Data Nucl. Data Tables 26 (1981) 477–481.
[39] E. Haug, Z. Naturforsch. 30a (1975) 1099–1113.
[40] L. Kim, R.H. Pratt, S.M. Seltzer, M.J. Berger, Phys. Rev. A 33 (1986) 3002–3009.
[41] M.J. Berger, S.M. Seltzer, Stopping power of electrons and positrons, Tech. Rep. NBSIR 82-2550, National Bureau of Standards, Gaithersburg, MD, 1982.
[42] M.J. Berger ESTAR, PSTAR and ASTAR: computer programs for calculating stopping-power and range tables for electrons, protons and helium ions, Tech. Rep. NISTIR 4999, National Institute of Standards and Technology, Gaithersburg, MD, 1992, available from www.nist.gov/pml/data/star/index.cfm.